# Journal Pre-proof

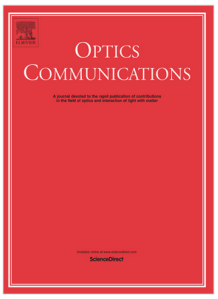


A dual-band frequency scanning antenna based on spoof SPPs transmission line

Panpeng Ge, Zhen Wang, Xiao Tu, Minran Lu, Ge Fan, Binggang Xiao

PII: S0030-4018(22)00480-1
DOI: https://doi.org/10.1016/j.optcom.2022.128743
Reference: OPTICS 128743

To appear in: *Optics Communications*

Received date : 11 April 2022
Revised date : 30 June 2022
Accepted date : 5 July 2022

Please cite this article as: P. Ge, Z. Wang, X. Tu et al., A dual-band frequency scanning antenna based on spoof SPPs transmission line, *Optics Communications* (2022), doi: https://doi.org/10.1016/j.optcom.2022.128743.

# A dual-band frequency scanning antenna based on spoof SPPs transmission line

Panpeng Ge[1], Zhen Wang[1], Xiao Tu[1], Minran Lu[1], Ge Fan[2], Binggang Xiao[1,*]

[1]*Key Laboratory of Electromagnetic Wave Information Technology and Metrology of Zhejiang Province, College of Information Engineering, China Jiliang University, Hangzhou 310018, China*

[2] *Southeast University, Nanjing 210096, China*

*bgxiao@cjlu.edu.cn

In this paper, a dual-band frequency scanning antenna based on spoof SPPs transmission line was proposed. The effect of each parameter in the rectangular holes of spoof SPPs on the dispersion characteristics and the frequency band of the spoof SPPs transmission line application was analyzed. The results show that the depths of rectangular hole have a large effect on the cut-off frequency, and etching two rectangular holes of different depths in a metal strip can generate standing waves in the transmission line. Based on this structure, a dual-band frequency scanning antenna was designed by combining magnetic coupling with the principle of leakage radiation. Loading two sets of circular patches of different sizes on both sides of the spoof SPPs transmission line achieved a dual-band frequency sweep of 90°- 196° in the 4-9 GHz and 126°-192° in the 16-32 GHz, with sweep angles of 106° and 66°. The antenna achieved a gain of 10-12 dBi in the operating band with an average radiation efficiency about 90%. The antenna was subjected to processing and testing, and the experimental results verified the good frequency scanning characteristics. The antenna proposed has a great potential for use in planar integrated communication systems and fifth-generation wireless communication system.

Keywords: Antennas; Spoof SPPs; Dual-band; Frequency scanning

## 1. Introduction

Surface plasmon polaritons (SPPs) is a mixed excited state of photons and electrons that propagates at the interface between metal and the medium, and it is capable of pushing the diffraction limit to the electromagnetic wave confined in the sub-wavelength range. In 2004, Pendry's team proposed the spoof SPPs structure, which enables surface plasmons to be applied to microwave and terahertz wave bands. The main way to achieve the spoof SPPs structure was to etch grooves in metal blocks to form metal grating structures[1]. Artificial SPPs have provided new ideas in microwave device research and miniaturization of microwave integrated circuits. Existing metal-etched corrugated structures in the sub-wavelength range have been extensively studied[2-6]. However, aforementioned structures were three-dimensional structures, which were not conducive to integrated processing and difficult to be applied in microwave integrated circuits. Therefore, Tiejun Cui's team proposed a two-dimensional planar ultra-thin sub-wavelength structure[7]. Rectangular grooves were periodically etched on the metal strips to form corrugated metal strips. The

structure could be printed on flexible dielectric substrates and be detached from the dielectric layer. The metal thickness of the structure was thin, making it easy to process and integrate. Subsequently, several studies on the integration from coplanar waveguide(CPW) or substrate were available. Substrate integrated waveguide(SIW) to Momentum-matching conversion structures for spoof SPPs were proposed[8,9]. Since then, artificial surface plasma metamaterials have been used in many microwaves band two-dimensional structured communication devices. Based on these developments, researchers have proposed other microwave band filters based on spoof SPPs structures[10-16], power dividers[17,18], couplers[19-21], antennas[22-27], and other communication devices. It has enriched the microwave band communication system and played a role in advancing the development of modern microwave communication circuits.

Leakage antenna has wide impedance bandwidth and high gain directional radiation characteristics, as well as strong directional and frequency scan characteristics[28]. Changing the antenna cell structure or adjusting the antenna operating frequency band, the direction of the antenna main flap radiation will also change. In recent years, in order to adapt to the trend of antenna structure miniaturization, planarization and integration, the research on the leakage antenna had also changed from rectangular waveguide. The basic structure of circular and metallic waveguides was shifting to planar. The leakage antenna based on artificial surface plasma feed was easy processing and manufacturing, easy planar circuit integration. The good performance and other characteristics have been widely studied in recent years.

The propagation constant of the spoof SPPs structure is greater than light at the same frequency and is capable of bringing the electric field. The beam is confined in the sub-wavelength range and propagates forward along the transmission line. However, when other structures are in close proximity, the electric field that is bound around the transmission line couples with them, breaking this constraint of the electromagnetic wave mode.

Based on the above principles, this paper proposed a dual-band frequency scanning antenna based on the spoof SPPs structure. The antenna was made by connecting metal gratings with rectangular holes of different etching depths in series, so that the spoof SPPs transmission line has two cut-off frequency. Loading specific sized circular patches equally spaced on both sides of the corresponding metal grating so that the antenna could realize isotropic radiation in both operating frequency bands. All of them were capable of frequency beam sweeping within a certain frequency range near their respective frequency points. Compared to previous scientific work, the proposed spoof SPPs based dual-band frequency sweep antenna achieves a frequency sweep at 4-9 GHz from 90° and 196° as well as from 126°-192° at 16-32 GHz. The scanning range of the two bands are 106° and 66°. And it has the advantages of simple structure and easy machining which plays a great value in limited volume integrated circuits.

## 2. Antenna Design and Analysis

### *2.1 Basic principle of leaky wave antenna*

According to the working mechanism of the antenna, leaky wave antennas are classified into uniform leaky wave antennas, quasi homogeneous leaky wave antennas and periodic leak wave antenna. The former two belong to fast wave radiation, periodic basic patterns for slow wave, leaky wave antenna can produce periodic disturbance space harmonic several times, including fast wave propagation will leak and energy[29,30]. Assuming that electromagnetic wave propagates in the z direction, the electric field $E_x(y,z)$ on the section of leaky wave structure (plane y=0) can be expressed as:

$$E_x(0,z) = Ae^{-jk_z z} \tag{1}$$

Where, $A$ is the constant representing the amplitude, $k_z$ is the complex propagation constant along the z direction, and its expression is:

$$k_z = \beta_z - j\alpha_z \tag{2}$$

Where， $\beta_z$ is the z-axis phase constant, $\alpha_z$ is the z-axis leakage wave constant. The electric field above the leaky wave structure can be expressed as:

$$E_x(y,z) = Ae^{-jk_z z}e^{-jk_y y} \tag{3}$$

Where , $k_y$ is the propagation constant along the y-axis, which can be expressed as:

$$k_y = \sqrt{k_0^2 - k_z^2} \tag{4}$$

Here, $k_z = \beta_z - j\alpha_z$ and the imaginary parts are equal, it can be concluded that:

$$\beta_z\alpha_z = -\beta_y\alpha_y \tag{5}$$

If the period of leaky wave antenna structure is infinite, $\theta$ represents the main direction of leaky wave antenna, then:

$$\cos\theta = \frac{\beta_z}{k_0} \tag{6}$$

As the frequency changes, $\beta_z$ and the main direction of leaky wave antenna structure changes along with the frequency, so leaky wave antenna has frequency scanning characteristics.

*2.2 Design of artificial surface plasma transmission line*

The spoof SPPs transmission line structure proposed in this paper consists of a dielectric substrate and a metal grating on the upper layer. Metal grating is formed by periodically etching rectangular holes on the metal strip, which enables the spoof SPPs transmission line to transmit artificial surface waves in the microwave frequency band, and the model structure is shown in Fig.1. Where h is the height of metal grating, p is the period of the rectangular aperture, d is the depth of the

rectangular hole, g is the width of the rectangular hole, $t_c$ is the thickness of the metal grating, and $t_s$ is the dielectric substrate thickness. The dielectric substrate thickness $t_s$ = 0.5mm, dielectric constant=2.65, and loss angle tangent is 0.003.

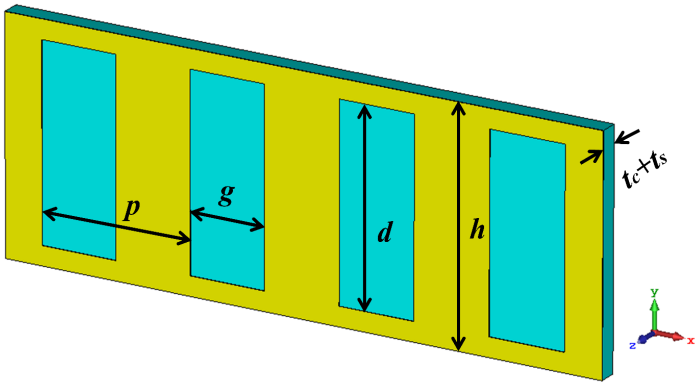


Fig.1. Schematic diagram of rectangular hole spoof SPPs structure

Compared with the traditional surface plasmon structure, spoof SPPs transmission line structure has an obvious characteristic. Its dispersion characteristics and restraint ability to electromagnetic field are affected by the parameter size of the structure. And it is concluded that the change of rectangular hole depth(d) has the greatest influence on the cut-off frequency of transmission line structure, which is consistent with the existing research results. In this paper, we use the electromagnetic field simulation software CST to calculate and analyze the influence of rectangular hole depth on the dispersion characteristics of spoof SPPs transmission line structure.

Fig.2 shows the dispersion curve of spoof SPPs transmission line structure corresponding to different rectangular hole depth d. The black solid line represents the propagation curve of light in the air, and other parameters are set as g = 2mm, p = 4mm, h = 10mm. From the Fig.2, it can be seen that with the increase of frequency, the wave vector of artificial surface gradually increases. And the dispersion curve gradually deviates from the light, tends to a stable value and reaches the cut-off frequency. This dispersion characteristic of spoof SPPs in the microwave band is similar to surface plasmas in the optical band. It shows that the spoof SPPs structure has the constraint ability to electromagnetic waves, which is similar to surface plasmon in optical band.

When d increases from 2mm to 9mm, the dispersion curve of the spoof SPPs structure deviates from the light, and the cut-off frequency decreases gradually. When d = 2mm, the cut-off frequency of the spoof SPPs structure is 34 GHz which means the artificial surface wave does not transmit when the frequency is higher than 34 GHz. And when d = 9mm, cut-off frequency decreases to 12.2 GHz. In this structure, when the frequency is higher than 12.2 GHz, the artificial surface wave stops transmitting. This property of the spoof SPPs structure can be used to connect metal gratings with different depths in series, thus allowing the same transmission line have two different cut-off frequencies.

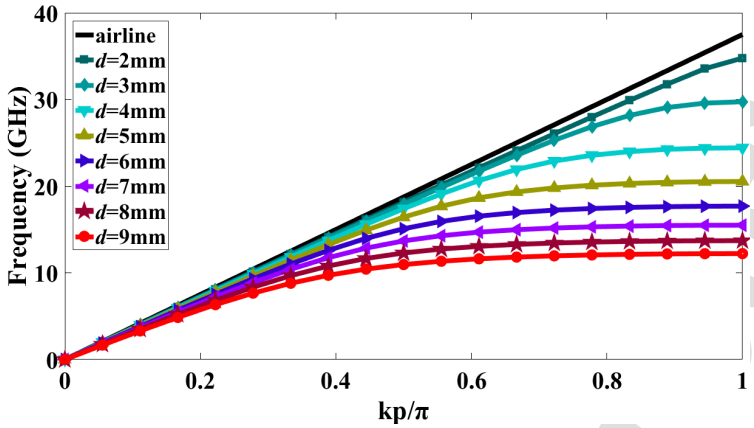


Fig.2. Effect of rectangular hole depth variation on dispersion curve

In the 2D planar structure, the conversion and bridging methods between coplanar waveguides, microstrip lines, SIW and spoof SPPs transmission lines have been proposed. In order to effectively excite the artificial surface plasma excitations and achieve impedance matching and mode conversion, this paper uses coplanar waveguide and spoof SPPs waveguide structure, the conversion structure proposed in this paper is based on the flare ground structure[8] and adaptive improvements based on it. The structural curve parameters is :

$$y = C_1 e^{\alpha x} + C_2 \tag{7}$$

Where $C_1 = \dfrac{y_2 - y_1}{e^{\alpha x_2} - e^{\alpha x_1}}$ , and $C_2 = \dfrac{y_2 e^{\alpha x_2} - y_1 e^{\alpha x_1}}{e^{\alpha x_2} - e^{\alpha x_1}}$ . In order to achieve impedance matching and mode matching between the waveguides, the parameters are optimized on the basis of the transmission line structure presented in this paper. The parameters of the final curve is:

$$y = a \times e^{\alpha x} \tag{8}$$

Where a=0.07, $\alpha$=0.1. The width of the center strip of the coplanar waveguide part $w_c$ = 9mm and the gap spacing $g_c$ = 0.25mm, as shown in Fig. 3.

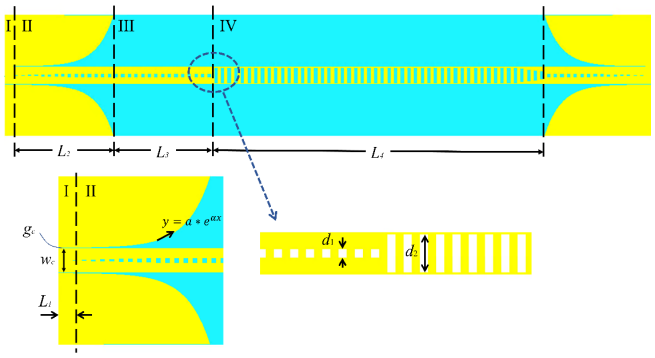


Fig.3. Schematic diagram of transmission line structure of spoof SPPs

The analysis of the dispersion characteristics of the spoof SPPs structure in the previous section shows that the depth of the rectangular hole affects the dispersion characteristics and cut-off frequency of the structure. Therefore, the depth of the rectangular aperture can be adjusted to control the operating frequency band. In addition, we use the cut-off frequency characteristics, connect two metal gratings with different depths of the rectangular in series. This design makes the transmission line has two cut-off frequency.

In this paper, we connect two rectangular hole metal with the depth of $d_1$ and $d_2$ in series. The resulting spoof SPPs transmission line structure is shown in Fig.3. In order to verify the effect of rectangular hole depth on the transmission performance of the transmission line, the effect of the rectangular hole depth $d_2$ variation on $S_{11}$ is given in Fig.4. It could be found that when the rectangular hole depth is changed from 6 mm to 9 mm, the impedance bandwidth is reduced from 18 GHz to 12 GHz. It is further verified that the rectangular hole depth variation has an effect on the cut-off frequency of the spoof SPPs structure and on the operating frequency band of the transmission line. As can be seen from the comparison between Fig.2 and Fig.3, the artificial surface waves propagate in a frequency band slightly smaller than the cut-off frequency, and in the design of this paper, since the size of $d_2$ in Part IV already determines the minimum cut-off frequency for this transmission line, $d_1$ will not discussed here. And based on this result , we set the depth of the etched rectangular hole $d_1$ = 2mm in region III, the etched rectangular hole in region IV depth $d_2$ = 9mm, rectangular hole width g = 2mm.

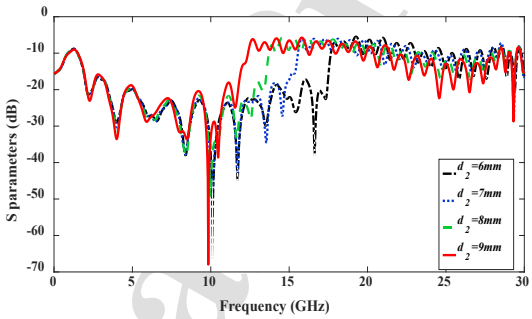


Fig.4. Effect of rectangular hole depth $d_2$ variation on spoof SPPs transmission line $S_{11}$

According to the analysis in Fig.2, when the frequency is lower than 12.2 GHz, the artificial surface wave propagates normally in the spoof SPPs transmission line structure. When the frequency band is between the cut-off frequencies of the two regions, the artificial surface wave propagates only in region III and cuts off in region IV. Therefore, if two waveguides are connected in series, a standing wave will be generated in region III. To validate the analysis, we use CST to get electric field distribution of spoof SPPs transmission line structures The electric field distributions at f = 5GHz, f = 10GHz and f = 15GHz, are given in Fig.5. It can be visualized that in the band below 12.2 GHz (at f = 5GHz, f = 10GHz), artificial surface waves are constrained near the waveguide structure and propagate along the transmission line. While in the band between the two cut-off frequencies (f = 15GHz), artificial surface waves in the band above the least cut-off frequency in this transmission line are cut off. And due to the presence of region IV, the propagation of artificial surface plasma waves is inhibited and standing waves are generated in region III.

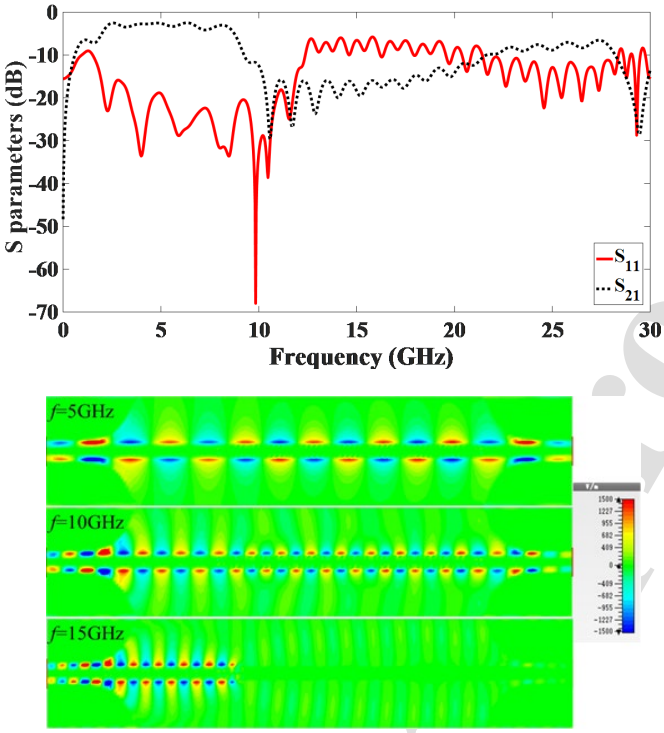


Fig.5. Electric field distribution of spoof SPPs transmission line structures (f = 5GHz; f =10GHz; f = 15GHz)

*2.3 Analysis and design of leaky wave radiation structure*

As can be seen from Fig.5, the spoof SPPs transmission line structure tightly limits the artificial surface wave near the structure and propagates along the transmission line below the cut-off frequency. In this section, a circular patch array structure is proposed, as shown in Fig6. This structure can convert the artificial surface wave constrained around the spoof SPPs transmission line structure into free space radiation wave. In this design, the spoof SPPs transmission line is used as the feeder, and the periodically arranged circular patch array is loaded on both sides of the transmission line, in which the patch array is divided into two groups. When the circular patch array is placed around the waveguide, the artificial surface wave is coupled to the patch and converted into radiation wave to radiate into free space.

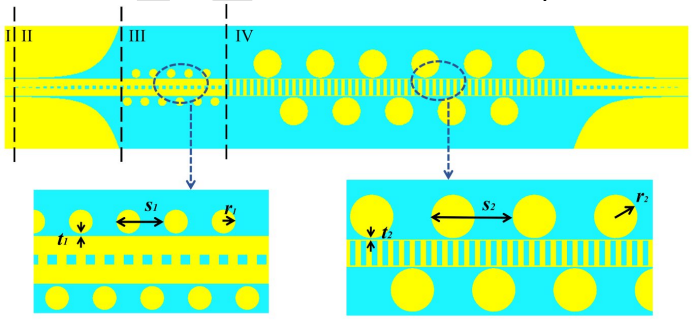


Fig.6. Schematic diagram of dual-band frequency scanning antenna fed by spoof SPPs

There are two coupling mechanisms for standing waves namely electrical coupling and magnetic coupling. Magnetic coupling occurs when the center of the circular patch array is at the maximum position of the magnetic field strength. Electrical coupling occurs when the center of the circle is located at the position of maximum electric field strength. In this section, magnetic coupling is used to feed the two circular patch arrays. Therefore, in this design, the center of the circular patch array should be located in the spoof SPPs transmission line magnetic field. The structure is magnetically coupled to the feeder at the location of maximum field strength.

Based on the above discussion, in order to ensure that every circular patch in the patch array is functional, the transmission line and the patch array should keep proper distance. If distance is too far, the current will not be fully coupled to the circular patch array. And if distance is too close, most of the energy will be associated with the front of the patch coupling results in the end patches not sensing the energy on the transmission line. Therefore, it is necessary to discuss the influence of the different spacing between the two groups of patch arrays and spoof SPPs transmission lines on the circuit characteristics and radiation performance of the antenna structure.

Since the circular patch array in region IV mainly affects the low-band radiation performance, the effect of $t_2$ is discussed here first in Fig.7. It can be seen in Fig.7, as $t_2$ increases from 0.5 mm to 2 mm, the antenna gain gradually decreases. When $t_2$=0.5 mm, the patch array is close to the feeder, it can better play the coupling role and make the antenna have better radiation characteristics.

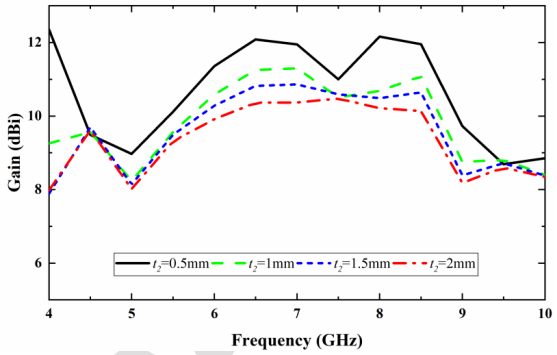


Fig.7. Change of $t_2$ versus gain

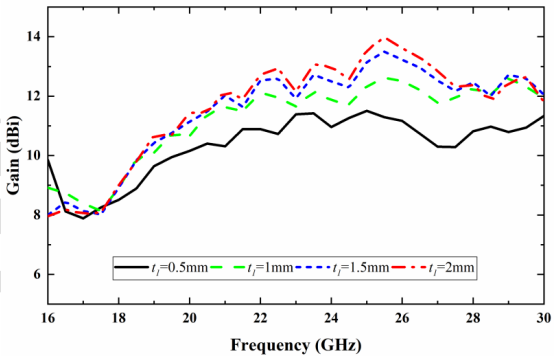


Fig.8. Change of $t_1$ versus gain

In the designed dual-band frequency-scanning antenna structure, patch array in region III mainly affects the frequency band in 16-30 GHz. The change of the antenna gain curve with $t_1$ is shown in Fig.8. It can be seen from the figure, when $t_1$ increased from 0.5mm to 2mm, the gain value of the antenna in the frequency band gradually increased. In addition to the gain curve, the influence of antenna also reflected in the radiation pattern at different frequency points in the frequency band. Fig.9 (a) and Fig.9(b) respectively show the direction of radiation at 16- 32 GHz for $t_1$ =2 mm and $t_1$=0.5 mm. From the comparison of the two figures, it is obvious that when $t_1$ = 0.5mm, the direction of the main lobe changes continuously with the change of frequency, which has the characteristic of frequency scanning. When $t_1$ = 2mm, there is no obvious polarization direction. It means that the patch array will only exhibit frequency beam scanning capability of the antenna structure with a short distance. Therefore, in the proposed design, the distance between the two patch arrays and the transmission lines of the spoof SPPs is set as $t_1$=$t_2$=0.5 mm.

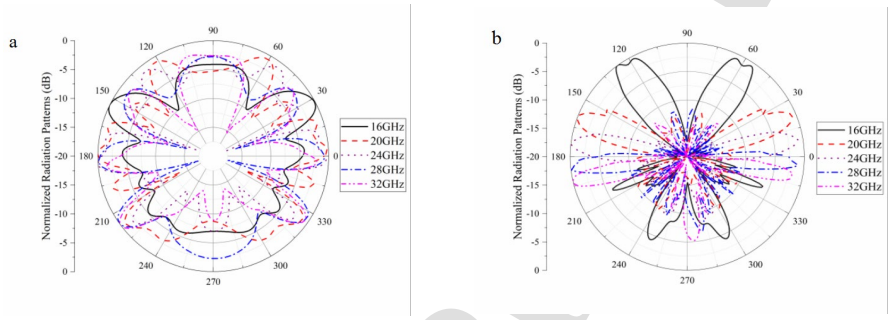


Fig.9. (a) 16-32 GHz different frequency direction diagrams at $t_1$=2mm (b) 16-32 GHz different frequency direction diagrams at $t_1$=0.5mm

In the designed antenna structure, the spoof SPPs transmission line plays the role of feed structure, and the artificial surface wave is tightly bound around the transmission line. The circular metal patch array is loaded near the transmission line to couple and excite the free space radiation wave. It takes two steps to transform the artificial surface wave transmitted in the spoof SPPs waveguide structure into free space. In the first step, the artificial surface wave constrained on the spoof SPPs transmission line is coupled to two groups of patch arrays by magnetic coupling. In this step, when the artificial surface plasmon is transmitted forward along the spoof SPPs transmission line, different positions on the transmission line have different phases. When the artificial surface wave on the waveguide is coupled to the circular patches in different positions, the phase difference between the patches will be introduced, which can be regarded as the compensation for the phase required in the second step. In the second step, the energy radiates through the circular patch array into free space, and due to the phase difference introduced between the patches, structure presents a frequency beam scan characteristic.

The directional diagrams of the main polarization of the dual-band frequency sweep antenna at different frequencies during vertical polarization are given in Fig.10 and Fig.11. Since the designed spoof SPPs frequency sweep antenna has no floor, the directional map is symmetrical with respect to the yoz face, and the axial realization of the patch array is frequency beam scanning. Fig.10 respectively shows the three-dimensional direction at 5-8 GHz. The beam scan from backward to forward is achieved. The two-dimensional radiation direction of the antenna in the two frequency

bands 4-9 GHz and 16-32 GHz are given in Fig.11. From Fig.11(a), it can be seen that in the 4-9 GHz band, the antenna radiates in the direction of 90°-196°, and the scan angle reaches 106°. Fig.11(b) gives the direction of the antenna radiation in the 16-32 GHz band at 126°-192° and the scan angle is 66°.

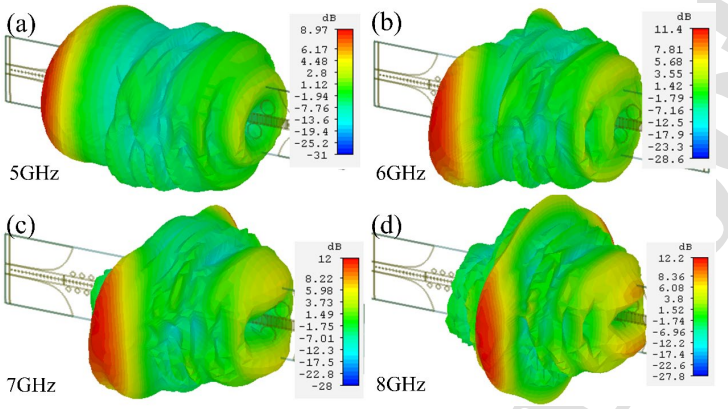


Fig.10. Three-dimensional orientation of the antenna at 5-8 GHz

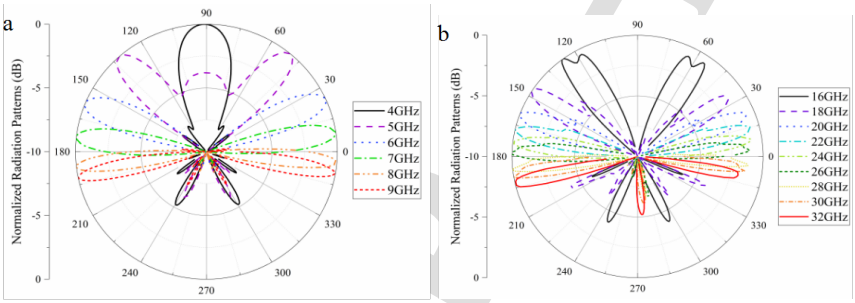


Fig.11. Normalized direction diagrams at different frequencies (a) 4-9 GHz; (b) 16-32 GHz.

## 3.Simulation and Measured Results

Processing of the proposed antenna structure is shown in Fig.12 based on the spoof SPPs dual-band frequency scanning antenna, the picture shows the front of the antenna, the ports on both sides are connected. We used K-joint, as the structure has no floor and the back side is an exposed substrate. The antenna S-parameter test environment is shown in Fig.13(a), and the test was performed using the Agilent N5230C vector network analyzer. The antenna radiation performance test environment is shown in Fig.13(b), which shows the antenna and standard gain during the test in the microwave dark room. The relative position of the horn antenna. Due to the limited frequency band of the vector network analyzer, only give the S parameter in the low frequency band of the antenna and far-field map test results here.

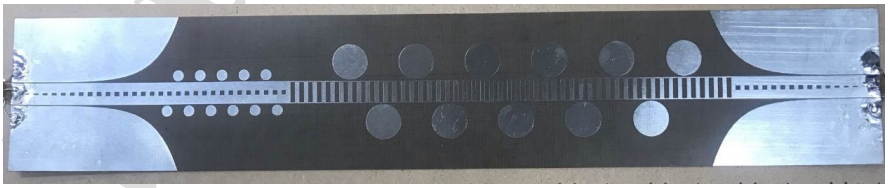

Fig.12. A fabricated sample of the proposed beam-scanning antenna

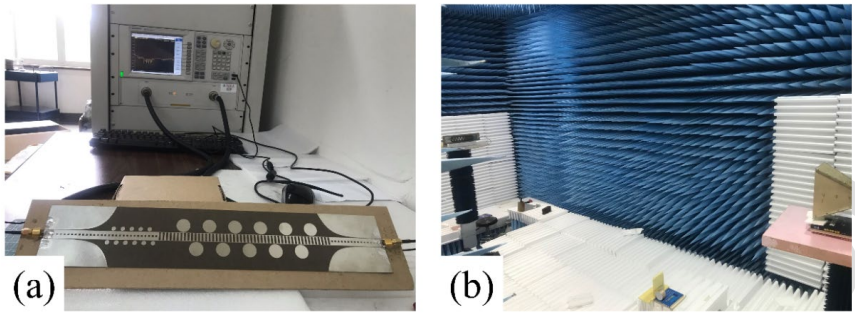


Fig.13. (a) Vector network analyzer test environment (b) Microwave anechoic chamber test environment

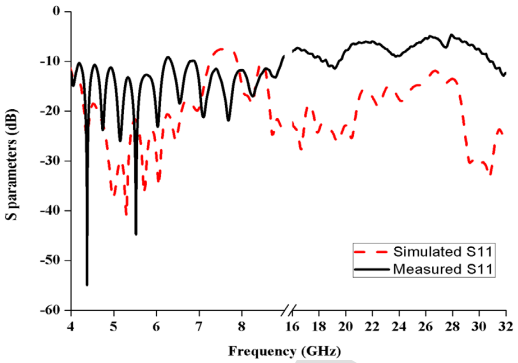


Fig.14. Simulation and Measured result of S11

Fig.14 gives the S11 simulation and test curves of the designed antenna. As shown in the figure, the dual band frequency sweep antenna based on the spoof SPPs meets $S_{11}$ < -10dB and impedance in the 4-9 GHz band in both simulation and test results. The bandwidth is almost identical. It can be seen that the deviation between the simulation and test results for $S_{11}$. The set-up of the simulation environment is ideal, but in the actual measurement, the fabricated processing of antenna and testing conditions also affected the final test results.

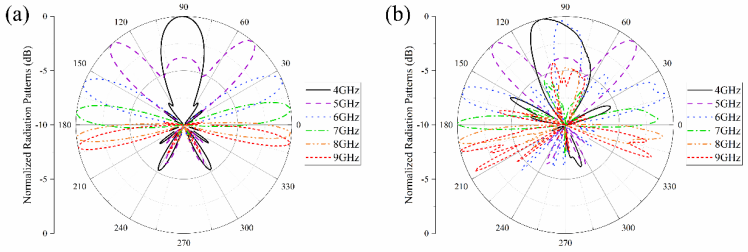


Fig.15. (a)(b)Simulation and Measured result of S11 at low frequency

The far-field direction diagram of the frequency sweep antenna in the 4-9 GHz band is shown in Fig.11, where the simulation results are shown in Fig.15(a), the test results are presented in Fig.15(b). The antenna corresponded to 90° and 196° main directions at 4-9 GHz, and 106° scanning range was achieved in this frequency band. The measured directional map is not perfectly symmetrical due to K-joint losses, antenna placement, and the influence of the turntable during the measurements. The scan angle and range in the test results of the antenna are close to the simulation results, indicating that the antenna has good frequency beam scanning characteristics.

## 4.Conclusion

The proposed spoof SPPs based dual-band frequency sweep antenna achieves a frequency sweep at 4-9 GHz from 90° and 196° as well as from 126°-192° at 16-32 GHz. The scanning range of the two bands are 106° and 66°. Simulation and experimental results consistently show that the antenna has a gain of 10-12 dBi in the operating band, with an average radiation efficiency of about 90%. The proposed frequency-scanning antenna is a two-dimensional planar structure, which has the advantages of simple structure, easy processing. Due to spoof SPPs are highly field strength-limited and can be integrated into other circuit structures in close proximity without coupling, which are advantages in the case of volume limited and is of great value in integrated circuits. The two frequency points of the antenna correspond to the two main application bands of the fifth generation of mobile communication technology, which can be used in planar integrated communication systems and fifth-generation wireless communication systems.

## Acknowledgments

This work was supported by 2021 Zhejiang Provincial Natural Science Foundation under Grant No. LY21F010012, and in part by 2016 Zhejiang Provincial Natural Science Foundation under Grant No.LY16F010010.

## References

[1]J. B. Pendry, L.Martín-Moreno, and F. J. Garcia-Vidal, “Mimicking surface plasmons with structured surfaces,” Science., vol 305, no. 5685, pp. 847-848, 2004.
[2]F. J. Garcia-Vidal, L. Martín-Moreno, and J.B. Pendry, “Surfaces with holes in them: New plasmonic metamaterials,” Journal of Optics A., vol 7, no. 2, pp. 97-101, 2005.
[3]A. P. Hibbins, B. R. Evans and J. R. Sambles, “Experimental Verification of Designer Surface Plasmons,” Science., vol 308, no. 5722, pp. 670-672, 2005.
[4]E. Moreno, S. G. Rodrigo, S. I. Bozhevolnyi et al., “Guiding and Focusing of Electromagnetic Fields with Wedge Plasmon Polaritons,” Physical Review Letters., vol 100, no. 2, pp. 023901, Jan. 2008.
[5]V. S. Volkov, S. I. Bozhevolnyi, S. G. Rodrigo et al. “Nanofocusing with channel plasmon polaritons,” Nano letters., vol 9, no. 3, pp. 1278-1282, 2009.
[6] A. I. Fernández-Domínguez, E. moreno, L. Martin-Moreno et al., “Guiding terahertz waves along subwavelength channels,” PHYSICAL REVIEW B., vol 79, no. 23, pp. 233104 , 2009.
[7]X. P. Shen, T. J. Cui, D. Martin-Cano et al., “Conformal surface plasmons propagating on ultrathin and flexible films,” Proc Natl Acad Sci USA., vol 110 , pp. 40-45, 2013.
[8]H. F. Ma, X. P. Shen, Q. Cheng et al., “Broadband and high-efficiency conversion from guided waves to spoof surface plasmon polaritons,” Laser & Photonics Reviews., vol 8, pp. 146-151, 2014.
[9]D. F. Guan, P. You, Q. F. Zhang et al., “Hybrid spoof surface plasmon polariton and substrate integrated waveguide transmission line and its application in filter,” IEEE Transactions on Microwave Theory and Techniques., vol 65, pp. 4925-4932, 2017.
[10]Q. Zhang, H. C. Zhang, H. Wu et al., “A Hybrid Circuit for Spoof Surface Plasmons and Spatial Waveguide Modes to Reach Controllable Band-Pass Filters,” Scientific Reports., vol 5, no. 1, pp. 494-521, 2015.
[11]K. Ogura, Y. Annaka, Y. Hoshi et al., “Spoof-Plasmon Instability in Terahertz Region Excited by Magnetized Electron Beam,” IEEE Transacyions on Plasma Science., vol 49, no.1, pp. 40-47, 2021.
[12]J. Xu, Z. Li, L. L. Liu et al., “Low-pass plasmonic filter and its miniaturization based on spoof surface plasmon polaritons,” Optics Communications., vol 372, pp. 155-159, 2016.
[13]Q. Zhang, T. Cui, “A series of compact rejection filters based on the interaction between spoof SPPs and CSRRs,” Science Letter., vol 6, no. 1, pp. 494-521, 2016.
[14]P. Chen, L. P. Li, K. Yang et al., “Hybrid Spoof Surface Plasmon Polariton and Substrate Integrated Waveguide Broadband Bandpass Filter With Wide Out-of-Band Rejection,” IEEE Microwave and Wireless Components Letters., vol 28, pp. 984-986, 2018.

[15]R. K. Jaiswal, N. Pandit, and N.P. Pathak, “Spoof Surface Plasmon Polaritons Based Reconfigurable Band-Pass Filter,” IEEE Photonics Technology Letters., vol 31, pp. 218-221, 2019.
[16]Z. X. Wang, H. C. Zhang, J. Y. Lu et al., “Compact filters with adjustable multi-band rejections based on spoof surface plasmon polaritons,” Journal of Physics D: Applied Physics., vol 52, no. 2, Jan. 2019.
[17]W. X. Tang, H.Z. Zhang, H.F. Ma et al., “Concept, Theory, Design, and Applications of Spoof Surface Plasmon Polaritons at Microwave Frequencies,” Advanced Optical Materials, vol 7, no.1, pp.1800421,2019.
[18]S. Y. Zhou, S. W. Wong, J. Y. Lin et al., “Four-Way Spoof Surface Plasmon Polaritons Splitter/Combiner,” IEEE Microwave and Wireless Components Letters., vol 29, pp.98-100, 2019.
[19]W. X. Tang, J. P. Wang, X. T. Yan et al., “Broadband and High-Efficiency Excitation of Spoof Surface Plasmon Polaritons Through Rectangular Waveguide,” Frontiers in Physics., vol 8, pp.582692, 2020.
[20]Y. Y. Meng, H. Ma, J. F. Wang et al., “BroadBand spoof surface plasmon polaritons coupler based on dispersion engineering of metamaterials,” Applied Physics Letters., vol 111, 2017.
[21]Y. T. Zhao, B. Wu, B. Y. Xue et al., “Ultrathin and flexible directional coupler with arbitrary coupling level using s-shaped spoof surface plasmon polariton coupled-line,” Applied Physics Express., vol 12 , pp.777, 2019.
[22]A. Kianinejad, Z. N. Chen, L. Zhang et al., “Spoof Plasmon-Based Slow-Wave Excitation of Dielectric Resonator Antennas,” IEEE Transactions on Antennas and Propagation., vol 64, pp. 2094-2099, 2016.
[23]G. S. Kong, H. F. Ma, B. G. Cai et al., “Continuous leaky-wave scanning using periodically modulated spoof plasmonic waveguide,” Sci Rep., vol 6, pp. 29600, 2016.
[24]D. F. Guan, P You, Q. F. Zhang et al., “A Wide-Angle and Circularly Polarized Beam-Scanning Antenna Based on Microstrip Spoof Surface Plasmon Polariton Transmission Line,” IEEE Antennas and Wireless Propagation Letters., vol 16, pp. 2538-2541, 2017.
[25]X. B. Liu, B. Chen, J. S. Zhang et al., “Frequency-Scanning Planar Antenna Based on Spoof Surface Plasmon Polariton,” IEEE Antennas and Wireless Propagation Letters., vol 16, pp. 165-168, 2017.
[26]Q. L. Zhang, Q. Zhang, and Y. Chen, “Spoof Surface Plasmon Polariton Leaky-Wave Antennas Using Periodically Loaded Patches Above PEC and AMC Ground Planes,” IEEE Antennas and Wireless Propagation Letters., vol 16, pp. 3014-3017, 2017.
[27]D. Tian, R. Xu, G. T. Peng et al., “Low-Profile High-Efficiency Bidirectional Endfire Antenna Based on Spoof Surface Plasmon Polaritons,” IEEE Antennas and Wireless Propagation Letters., vol 17, pp. 837-840, 2018.
[28]M. Kalantari, W. Li, H. Shirinabadi, A. Fotowat-Ahmady et al., “A W-Band Single-Antenna FMCW Radar Transceiver With Adaptive Leakage Cancellation,” IEEE Journal of Solid- State Circuits., vol 56, no.6, pp. 1655-1667, 2021.
[29]J. Wang, L. Zhao, Z. C. Hao et al., ”An ultra-thin coplanar waveguide filter based on spoof surface plasmon polaritons,” Applied Physics Letters, vol 16, pp.3014-3017, 2017.
[30]J. Liu, D. R. Jacson, Y. Li et al., ” Investigations of SIW Leaky-Wave Antenna for Endfire-Radiation With Narrow Beam and Sidelobe Suppression ,” IEEE Transactions on Antennas and Propagation, vol 62, no.9, pp.4489-4497, 2014.

## Declaration of Interest Statement

The authors declare that they have no known competing financial interests or personal relationships that could have appeared to influence the work reported in this paper.